

# MEASUREMENT AND PREDICTION OF CENTRIFUGAL COMPRESSOR AXIAL FORCES DURING SURGE: PART 1 – SURGE FORCE MEASUREMENTS

Klaus Brun<sup>1</sup>, Sarah Simons<sup>1</sup>, Rainer Kurz<sup>2</sup>, Michele Pinelli<sup>3</sup>, Mirko Morini<sup>4</sup>, Enrico Munari<sup>3</sup>

1 Southwest Research Institutes, San Antonio, Texas, USA

2 Solar Turbines, Inc., San Diego, California, USA

3 Dipartimento di Ingegneria, Università degli Studi di Ferrara, Ferrara, Italy

4 Dipartimento di Ingegneria Industriale, Università degli Studi di Parma, Parma, Italy

[klaus.brun@swri.org](mailto:klaus.brun@swri.org)

[sarah.simons@swri.org](mailto:sarah.simons@swri.org)

[Kurz\\_Rainer\\_X@solarturbines.com](mailto:Kurz_Rainer_X@solarturbines.com)

[michele.pinelli@unife.it](mailto:michele.pinelli@unife.it)

[mirko.morini@unipr.it](mailto:mirko.morini@unipr.it)

[enrico.munari@unife.it](mailto:enrico.munari@unife.it)

## ABSTRACT

Centrifugal compressor impellers and shafts are subject to severe fluctuating axial and radial forces when operating in surge. These forces can cause severe damage to the close clearance components of a centrifugal compressor such as the thrust and radial bearings, inter-stage and dry gas seals, and balance piston. Being able to accurately quantify the cyclic surge forces on the close clearance components of the compressor allows the user to determine whether an accidental surge event, or emergency shutdown (ESD) transient, has caused damage requiring inspection, repair, or part replacement. For the test, a 700 Hp (~520 kW) industrial air centrifugal compressor was operated in surge at speeds ranging from 7,000 to 13,000 rpm and pressure ratios from 1.2 to 1.8. The axial surge forces were directly measured using axial load cells on the thrust bearings. Suction and discharge pressures, proximity probe axial shaft position, flows, and temperatures were also measured. Time domain and frequency plots of axial vibration and dynamic pulsations showed the impact of the operating conditions on surge force amplitudes and frequencies. A surge severity coefficient was also derived as a simple screening tool to evaluate the magnitude of potential damage to a compressor during surge.

## KEYWORDS

Surge. Compressor. Transient Flow.

## INTRODUCTION

The typical centrifugal compressor performance map (head or pressure ratio versus flow rate) with the corresponding speed lines indicates there are two (2) limits on the operating range of the compressor. Global aerodynamic flow instability, known as surge, sets the limit for low-flow (or high-pressure ratio) operation while choke or “stonewall” sets the high flow limit [1]. The exact location of the surge line on the map can vary depending on the operating condition and, as a result, a typical safe surge margin (expressed as a percentage difference between the design flow and the flow surge limit, at the same corrected rotational speed, see also API 617 requirements and stability margin) is established above the stated flow for the theoretical surge line. Most centrifugal compressor manufacturers design the machine to have at least 15% surge margin during normal operation and set a recycle valve control line at approximately 10% surge margin (if the working fluid is natural gas, recycle is needed, whereas if it's air, a simple blow off system is required). That is, once surge margin falls below 10%, the recycle valve is opened to keep the compressor operating above the 10% surge margin line. Thus, every turbo-compressor has a limiting point of stability on its operating map. Once this point is reached, at a certain rotational speed, surge can occur, resulting in a breakdown and in cyclical flow and pressure pulsations in the compressor (these pulsations can be so violent and lead to flow-reversal - this is called deep surge).

Surge occurs just below the minimum flow that the compressor can sustain against the existing suction to discharge pressure rise (head). Once deep surge occurs, the flow reversal reduces the discharge pressure or increases the suction pressure, thus allowing forward flow to resume until the pressure rise again reaches the surge point. This surge cycle continues at a low frequency until some change takes place in the process or the compressor conditions. The frequency and magnitude of the surge flow-reversing cycle depend on the design and operating condition of the machine, but in many cases it is sufficient to cause damage to the seals and bearings and sometimes even the shaft and impellers of the machine.

Surge is a global instability in a compressor's flow that results in a complete breakdown and, in case of deep surge, generates flow reversal through the compressor. The classic compressor head-flow performance map, or the nondimensionalized psi-phi curves [2], is appropriate for the characterization of steady-state and slowly changing operating conditions, but it is not fully applicable for rapidly transient compressor flow conditions [3]. Since surge is a highly transient phenomenon that involves pressure differentials across the compressor, both the surge flow frequency and amplitude are strong functions not only of the compressor but also of the associated piping system, as confirmed in the work of Sparks [4]. For example, FIGURE\_16 shows a plot of the measured surge frequency versus

pipng discharge volume (compressor discharge flange to check valve) for the low pressure air compressor tested and described in the paper herein. The plot also shows peak-to-peak axial force versus piping discharge volume.

Several measurements were done by varying the downstream volume. In this paper only the results @ 9,000 rpm are shown. In this piping system, decreasing the discharge volume results in a significant increase in the surge frequency from 0.25 Hz to 3.5 Hz. Clearly, for a given compressor and associated piping system, the surge frequency and amplitude is machine and system specific.

Surge forces often result in severe damage to close clearance components of a centrifugal compressor such as the thrust and radial bearings, inter-stage and dry gas seals, and balance piston. In a compressor (no unbalance, no misalignments, and no rubs), surge, which is an axial-symmetric phenomenon, causes some radial vibration (minor) and high axial displacements, due to cyclic thrust reversal. Therefore, the strongest surge forces are those in the axial direction and the highest risk of failure component is the compressor's axial thrust bearing. Although in severe cases even the impellers can be damaged (see FIGURE\_).

Knowledge of the amplitude and frequency of the unsteady axial surge forces is imperative to predict the extent of wear or failure that will occur from surge overload cycle fatigue conditions. This paper develops a method to quantify the cyclic axial surge forces on the close clearance components of the compressor thus allowing the user to determine whether an accidental (or ESD transient) surge event causes sufficient damage to require inspection, repair, or part replacement. For this work, experimental surge testing was performed using an industrial centrifugal compressor operating in an open cycle air configuration.

The experimental data was then compared and validated with a transient 1-D lump sum parameter model of the compressor system [5]. Details of the test setup, the measurement results, transient modeling approach, code implementation, and comparisons between analysis and testing are provided herein.

## **BACKGROUND**

Centrifugal compressor systems are often exposed to surge events, during startup, shut down, accidentally or during ESD events. Being able to quantify the forces on close clearance components and the resulting potential damage that occurs to those components of the compressor provides significant value in:

- Determining if an accidental surge event caused damage without having to perform costly inspections.
- Determining if and how frequently close clearance parts should be inspected and replaced after multiple ESD surge events.
- Evaluating whether a compressor can be operated for limited periods in surge to allow for optimal and safe ESD sequencing.
- Designing compressor close clearance components that can withstand surge events for extended periods of time.

Currently, no validated method exists to predict the frequency and amplitude of the forces to determine extent of wear or potential for failure of these components.

Surge in centrifugal compressors has been studied by a number of researchers over the last 120 years [6-8]. It is beyond the scope of this paper to list all of them, but a good summary review of the centrifugal compressor surge phenomenon can be found in [9] and in [10]. Recently, Moore, et al. [11] numerically analyzed the rotordynamic force which generate in centrifugal compressor impellers during operation. However, few researchers have modeled and investigated the surge event to predict surge force frequency and amplitudes.

In 1976, Greitzer [12, 13] studied surge and rotating stall in axial flow compressors and performed a theoretical study of axial compressor surge. Numerical results are presented to show the motion of the compression system operating point during these two (2) basic modes of instability, and a physical explanation is given for the mechanism associated with the generation of surge cycle oscillations. Greitzer also reported on an experimental study of axial compressor surge and rotating stall. The model is shown to provide an adequate quantitative description of the motion of the compression system operating point during the transients that occur subsequent to the onset of axial compressor stall.

In 1981, Hansen, et al. [14] performed an experimental and theoretical study of surge in a small centrifugal compressor. Experimental results for deep surge in a small single-stage centrifugal compressor are compared to predictions based on the lumped parameter Greitzer model developed for axial compressors. The stability limit of the model equations were also studied for finite amplitude disturbances. Successively, the Greitzer's model was extended by Fink, et al. [15] who introduce the treatment of the speed velocity together with the time lag related to the through flow time. In the same period, Botros [16] examined the transient phenomena in compressor stations during surge and discovered transient phenomena are generally inherent in the operation of compressor stations. It was found that by keeping the recycle valve closed upon shutdown, the rate of shaft deceleration will be reduced.

In recent years, many investigators continue to propose new models [17-23]. Yoon, et al. [17] studied an enhanced Greitzer compressor model including pipeline dynamics and surge. Their work included the modeling of a centrifugal compressor system with exhaust and plenum piping acoustics. Good agreement was observed between the experimental and theoretical frequency responses from the tip clearance to the output pressure, both in stable operation and during surge. Hiradate, et al. [18] investigated pressure fluctuations related to mild surge in multi-stage centrifugal blowers with inlet guide vanes. Their work showed that pressure fluctuation under the IGVs partially open condition were caused by the mild surge due to the positive slope of the pressure-rise characteristic at the second to the last stages. It was also found that this mild surge was caused by the stall of the vaned diffusers at the second to the last stage. Dumas, et al. [19] performed the post-surge load predictions for multi-stage compressors via CFD simulations. They proposed a methodology for the simulation of post-surge condition in multi-stage compressors that are part of a gas generator system and also include the combustor

and turbine and ducts. A comparison of predicted versus measured shaft loading amplitude during surge showed good agreement. Belardini, et al. [20] modeled pressure dynamics during surge and ESD. Their results obtained showed good agreement with pressure and speed trends measurement from field testing. Biliotti, et al. [21] evaluated stall induced aerodynamic forcing and rotor vibrations in a multistage centrifugal compressor. The calculated stall force was used as an input into a rotordynamic model of the whole compressor. The predicted Subsynchronous Vibration (SSV) estimated at the displacement probe location was also compared with the measured values. Baldanzini, et al. [22] performed exploration tests and second quadrant characteristic dynamic modeling of centrifugal compressors. Surge exploration test results analyzed in terms of vibrations and thrust loads, together with development of a compressor enhanced dynamic model, allowed the move from a surge acceptance criterion based on the time spent on the left of the Surge Limit Line during an Emergency Shutdown event to a more physics based criterion based on the acceptable number of surge cycles. Recently, Munari, et al. [23] developed a dynamic model based on the bond graph approach demonstrating its reliability in simulating deep surge fluctuations by means of a comparison with the experimental data obtained in Munari et al. [24].

Although several authors investigated the forces created during a surge event in a centrifugal compressor, there is no test data available in the public domain where such a model is actually compared to laboratory quality test data. Within this project, high fidelity fluctuating forces, pressures, and temperatures were taken at the suction and discharge of an industrial centrifugal compressor for multiple speed line surge conditions. This detailed test data is compared to predictions from a lump parameter bond-graph method dynamic analysis. Also, a surge severity coefficient is derived that can be utilized as a screening tool to determine the magnitude of potential damage to the compressor during a surge event.

## **TEST SETUP**

Laboratory testing centrifugal compressor surge operation was performed in an air loop at the SwRI centrifugal compressor laboratory. FIGURE\_ shows a photo of the compressor and test arrangement. The compressor has two (2) impeller stages and has a horizontally split casing. TABLE 6 reports the main characteristic of the compressor stages.

The facility allows for open, semi-open, and closed loop operation. Open loop operation was chosen for the subject testing to best control flow and pressures at low loop process pressures. The driver is a 700 hp (~520 kW) variable speed electric motor. Flow and head of the compressor is controlled using a discharge throttle valve. For the testing the machine speed was varied from 7,000 to 13,000 rpm at 1,000 rpm intervals, avoiding a critical speed near 8,000 rpm. Although a recycle valve and discharge cooler were available on this loop, they were not utilized for the testing presented herein. The highest pressure ratio at the highest speed line was 1.75. The centrifugal compressor's performance map recorded for this test, including the measured surge line, is shown in FIGURE\_ As can be seen, the surge line does not coincide with the minimum flow rate at each specific curve – as typically represented in performance maps of compressors. In fact, in this work steady-state tests and surge tests were carried out separately. Since the raw test data and reduced

results produced herein are intended to be open to the industry for benchmarking, code validation, and design comparison, a detailed test loop process and instrumentation diagram (P&ID) is included in FIGURE\_ with all relevant piping dimensions. To reduce overall measurement uncertainty (as can be seen in the P&ID in FIGURE\_), flow, pressure, and temperature measurements were installed in the test loop per ASME PTC-10 requirements. Instrumentation included four (4) static pressure and three (3) temperature measurements mounted on the inlet and outlet compressor nozzles as well as in additional locations throughout the piping, steady-state flow measurement from an orifice plate meter in the main piping, x/y/z proximity probes on the bearings, and bearing temperature measurements. To obtain high accuracy axial thrust force measurements, three (3) fast respond high fidelity load cells were mounted directly onto the thrust bearings as shown in FIGURE\_. TABLE 7 the main characteristics of the instrumentation used are reported.

Rotor surge force measurements can thus be obtained three (3) different ways:

- Direct measurements from the load cells on the axial thrust bearings
- Integration of the proximity probe displacement and thrust bearing stiffness:

$$F(t) = \int k(t)dx \quad (1)$$

- Integration of the impeller surface area with the pressure measurements:

$$F(t) = \int p(t)dA \quad (2)$$

The first two methods were used for data evaluation of the testing described herein. The last method of the list is most applicable the force determination from numerical analysis. Without a dedicated load cell the only method that can be used (e.g., for field measurements) would be method 2 but the uncertainty of this approach would be relatively high because of variances in bearing stiffness. All individual instruments were calibrated prior to the test to manufacturer's accuracy requirements. End-to-end calibrations with all data acquisition systems included were also performed. Total measurement and data acquisition uncertainties were predicted using the perturbation method and validated versus data scatter. Typical uncertainties for raw and reduced parameters are shown in TABLE 8 as percent deviation from the operating point.

## TEST PROCEDURE

Prior to the surge testing, the ability to identify and measure the onset of full surge needed to be validated. Specifically, the location of the surge line across the compressor head-flow map was verified. Critical instrumentation for surge identifications are thrust bearing proximity probes, suction/discharge unsteady pressures, and axial thrust load cells. Significant increases in axial thrust vibrations as well as pulsations were seen for the compressor at all speed lines. For example FIGURE\_ shows axial shaft vibrations of the compressor

for the 13,000 rpm speed line just to the right of the surge line (no surge) and in full surge. Similar results were obtained for all operating conditions of the compressor. Surge for this machine and associated piping system is generally observed between 2.25 to 3.5 Hz for a fixed discharge volume ending at the primary discharge control valve in the system.

For the surge testing the machine was operated in full surge (i.e., just to the left of the surge line and when full surge was detected from the instrumentation) for the speeds between 7,000 and 13,000 rpm at 1,000 rpm increments. The only speed that was omitted was at 8,000 rpm since it corresponded closely to the lateral first critical speed of the rotor.

## TEST RESULTS AND ANALYSIS

Vibrations, pulsation, and load test data was analyzed for each of the surge test points. For example, FIGURE\_ and FIGURE\_ show surge peak-to-peak proximity probe oscillations and pressure pulsations, respectively. Significant surge dynamics can be seen between 2.25 to 2.5 Hz. However, for a quantitative comparison to simulation prediction results, the most relevant data measurements are the axial thrust forces from the load cells. Since these are direct force measurements (unlike the force estimates derived from equations (1) and (2)) they represent the most accurate data for comparisons.

FIGURE\_ shows load cell measurement results for the 13,000 rpm speed line surge case (raw dynamic axial load data are not shown in this paper).

Low-pass filtered data (<25 Hz) is plotted versus time. Both the non-surge and the full surge cases are presented. Axial force amplitudes of 25 lbf (~111 N, peak-to-peak) for the surge case and 8 lbf (~35 N) for the non-surge case can be seen. For the non-surge case the axial forces are fairly broadband, but when further bandpass filtering is applied to the data between 2-4 Hz to eliminate spurious noise, the axial forces for the non-surge case approach zero. The surge case data can be further post-processed into the frequency domain showing the characteristic surge frequency at 2.5 Hz (FIGURE\_). One should note that this plot shows zero-to-peak data and, to obtain the correct total force magnitudes, the first 2.5 Hz order and multiple higher orders have to be added. Similar results were obtained for all speed line surge and non-surge cases. These can be combined into a single plot as shown in FIGURE\_. Specifically, FIGURE\_ shows a plot of surge forces versus speed for all test cases.

As expected axial vibration peak-to-peak forces at the surge frequency increase with speed and, thus, also with pressure ratio. The difference between steady-state (not surge) and surge axial forces versus compressor pressure ratio can be seen in FIGURE\_. A trend-line (dotted) is also presented. Although insufficient statistical data is available for a definite polynomial trend analysis, the impact of the surge event on the unsteady forces of the compressor appears to be approximately linearly related to compressor pressure ratio.

Similarly, FIGURE\_ shows peak-to-peak vibrations during surge versus the compressor speed with a curve-fit trend-line. Again, a near linear trend can be observed. As previously discussed, from the proximity probe vibration data the axial forces can also be indirectly

calculated by integrating them with the thrust bearing tilt pad stiffness as shown in FIGURE\_. Results from these calculations were within 15% of the direct axial load cell measurement. Clearly, the load cell data is a direct measurement and is considered to be more accurate; therefore it was used for data analysis and comparison to simulation predictions.

FIGURE\_-FIGURE\_ show a somewhat irregular trend in a specific range of rotational speeds (9,000 - 11,000 rpm) which does not agree with general linear trend. This is due to (i) the difficulties and uncertainty of these type of measurements - the complexity of these measures is due to many factors: vibration of the system, measurement noise, repetitiveness of tests, etc. - and (ii) the different degree of surge generated during tests at the different rotational speeds (the degree of surge strongly depends on the relation between rotational speed and valve closure). Based on these considerations, the linear trend approximation might be considered valid.

Finally, FIGURE\_ shows surge frequency as a function of speed. The frequency is seen to decrease with increasing speed but levels out asymptotically at approximately 2.5 Hz.

As seen in FIGURE\_, compressor surge frequency is a strong function of compressor discharge volume (between discharge flange and check valve) and only a weak function of compressor speed.

## DATA REVIEW

As an initial screening test to determine the severity of a surge event, a surge severity coefficient was derived based on energy conservation non-dimensional analysis. The term “severity” indicates the magnitude of potential damage of surge events. In other words,  $\Gamma$  evaluates how severe the damage can be in the compressor (or in general, in compressor components) produced by a surge event. This is different from the Greitzer’s parameter,  $B$ , which instead defines the type of instability, rotating stall or surge, which is likely to occur in the system. The herein proposed parameter,  $\Gamma$ , considers the individual energy contributions that impact the magnitude of the energy transferred to the rotor are lumped into a single non-dimensional parameter,  $\Gamma$ . These energy contributions are either causative (they lead to surge), such as the discharge gas pressure-volume and the force-movement of the impeller, or restorative (they favor a steady operating point) such as the enthalpy rise produced by the compressor, the mass inertia of the rotor, and the stiffness reaction of the bearings. The surge severity coefficient,  $\Gamma$ , was thus defined as:

$$\Gamma = \frac{r^2 \cdot V \cdot \Delta P^2}{s \cdot m \cdot k \cdot \Delta h} \quad (3)$$

This coefficient takes into account the main parameters which affect the potential damage due to surge event (in this sense the authors called it “Severity Coefficient”). It has been obtained by means of a preliminary simple energy-based non-dimensional analysis and then by heuristically rearrange the terms on a phenomenological observation basis.



This coefficient does not replace a full dynamic analysis of the rotor and compressor system but can be used as an initial screening tool to estimate the severity of a surge event. Specifically, for a given class and geometry of a compressor, for a high  $\Gamma$  the surge forces will generally be more severe than for a small  $\Gamma$ . For the surge test data described above the surge severity coefficient was calculated and results are presented in TABLE 9. The actual level of  $\Gamma$  at which damage occurs is clearly machine and geometry dependent. However, from basic hand-calculations of resultant forces one can estimate that surge events with  $\Gamma > 0.01$  have a strong potential to result in damage and should be further investigated. Similarly, surge events with  $\Gamma < 0.001$  are mild and will likely not cause machine damage (see

TABLE 10). The tested surge cases  $\Gamma$ 's were all well below 0.001 and no damage was seen on the compressor.

One should note that, due to the limited availability of data, these surge severity coefficient ranges are likely only valid for this type, application, and geometry of centrifugal compressors. Care should be taken when attempting to generalize these findings to other compressors.

## **SUMMARY AND CONCLUSIONS**

Centrifugal compressors experience severe unsteady forces when operating in surge. These forces can cause damage to the close clearance components. Although several authors have theoretically investigated the forces created during a surge event in a centrifugal compressor, there is no test data available in the public domain where such a model is actually compared to laboratory quality test data. To address this knowledge gap, full surge tests on an 700 hp (~520 kW) industrial scale centrifugal compressor were performed over speeds ranging from 7,000 to 13,000 rpm and pressure ratios from 1.2 to 1.8. During surge the forces in the axial direction are the most severe, and the thrust bearing has the highest risk for failure. Consequently, high fidelity unsteady axial surge forces were directly measured using axial load cells on the thrust bearings. Suction and discharge the dynamics of pressures, proximity probe axial shaft position, flows, and temperatures were also measured for comparison calculations. Time domain and frequency plots of axial vibration showed the impact of the operating conditions on surge force amplitudes and frequencies. The measurement results from this testing can be used for comparison and validation of dynamic surge models and to identify the potential damage of close axial clearance components. Specific conclusions from the testing are:

- Axial surge forces are seen to increase near linearly with the operating speed and pressure ratio of the compressor.
- Surge frequency is a strong function of discharge volume and a very weak function of operating speed.
- Test results from the axial load cells compared to forces derived from integrating bearing stiffness coefficients with proximity probe displacement data.

A surge severity coefficient was derived as a simple screening tool to evaluate the potential damage to a compressor during surge. Surge severity coefficients below 0.001 are generally mild while coefficients above 0.01 are strong and can lead to damage for the tested type of compressor, geometry, and application.

Results from this work can help centrifugal compressor operators to directly assess the risk of close clearance component potential damage during a surge event. For example, conventional compressor station design wisdom holds that reduced discharge volume is better to avoid transient surge. However, this is not true for all design cases. While there is less energy in surge, the surge may occur at a frequency that could potentially be more damaging to the compressor. Thus, the correct compressor station piping design should take the severity of possible transient surge events into account.

Also, in Part 2 of this paper the detailed test data is used to validate a lumped parameter dynamic compressor analysis for prediction of surge forces on a wider range of centrifugal compressor models.

## **ACKNOWLEDGMENT**

The authors would like to thank the Southern Gas Association and Gas Machinery Research Council for the financial support of this project and the technical guidance they provided.

## **NOMENCLATURE**

$d$  - displacement

$k$  - axial thrust bearing stiffness

$m$  - mass of the rotor

$N$  - rotational speed

$p$  - Pressure

$Q$  - actual flow

$r$  - impeller tip radius

$s$  - axial thrust bearing normal operational clearance

$T$  - temperature

$V$  - compressor discharge flange to check valve volume

$\Delta h$  - compressor enthalpy rise (head)

$\Delta P$  - pressure difference across compressor (Pd - Ps)

## REFERENCES

- [1] Japikse, D. "Centrifugal compressor design and performance". (1996) Wilder, VT: Concepts ETI, Inc.
- [2] Shapiro, L. "Performance Formulas for Centrifugal Compressors". (1996) Solar Turbines Publication, San Diego, CA
- [3] Brun, K. and Kurz, R. "Analysis of the Effects of Pulsations on the Operational Stability of Centrifugal Compressors in Mixed Reciprocating and Centrifugal Compressor Stations". (2010) *Journal of Engineering for Gas Turbines and Power*, vol. 132, n 7.
- [4] Sparks, C. R. "On the Transient Interaction of Centrifugal Compressors and Their Piping Systems". (1983) ASME International Gas Turbine Conference and Exhibit, 83-GT-236, pp. V003T07A016-V003T07A016.
- [5] Munari, E., Morini, M., Pinelli, M., Brun, K., Kurz, R., Simons, S. "Measurement and Prediction of Centrifugal Compressor Axial Forces During Surge: Part 2 – Dynamic Surge Model", (2017), GT2017-63070.
- [6] Morini, M., Pinelli, M., Venturini, M. "Development of a One-Dimensional Modular Dynamic Model for the Simulation of Surge in Compression Systems". (2006) *Journal of Turbomachinery*, 129 (3), pp. 437-447.
- [7] Aust, N. "Ein Verfahren zur digitalen Simulation instationaerer Vorgaenge in Verdichteranlagen". (1988) Diss U Bw, Hamburg.
- [8] Wachter, J., Loehle, M. "Identifikation des dynamischen Uebertragungsverhaltens eines dreistufigen Radialverdichters bei saug- und druckseitiger Durchsatzvariation". (1985) VDI Bericht 572.2, pp. 365-379.
- [9] Kurz, R., McKee, R., Brun, K. "Pulsations in Centrifugal Compressor Installations". (2006) *Proceeding of ASME TurboExpo*, GT2006-90700, pp. 535-542
- [10] Brun, K. and Nored, M. "Application Guidelines for Surge Control System". (2008) Gas Machinery Research Council Publication, Dallas, TX.
- [11] Moore, J.J., Ransom, D.L., Viana, F. "Rotordynamic force of centrifugal compressor impellers using computational fluid dynamics". (2010) *J. Eng. Gas Turbines Power*, 133(4), 042504, doi:10.1115/1.2900958.
- [12] Greitzer, E.M. "Surge and Rotating Stall in Axial Flow Compressors – Part I: Theoretical Compression System Model". (1976) *Journal of Engineering for Power*, 98(2), pp. 190-198.
- [13] Greitzer, E.M. "Surge and Rotating Stall in Axial Flow Compressors – Part II: Experimental Results and Comparison with Theory". (1976) *Journal of Engineering for Power*, 98(2) pp. 199-217.

- [14] Hansen, K.E., Jorgensen, P., Larsen, P. S. "Experimental and Theoretical Study of Surge in a Small Centrifugal Compressor". (1981) *Journal of Fluids Engineering*, Vol. 103, pp. 391-395.
- [15] Fink, D.A., Cumpsty, N.A., Greitzer, E.M. "Surge Dynamics in a Free-spool Centrifugal Compressor System". (1992) *J. Turbomach* 114(2), pp. 321-332, doi:10.1115/1.2929146.
- [16] Botros, K.K. "Transient Phenomena in Compressor Stations During Surge". (1994) *Journal of Engineering for Gas Turbines and Power*, Vol. 116, pp. 133-142.
- [17] Yoon, S. Y., Lin, Z., Goynes, C., Allaire, P. "An Enhanced Greitzer Compressor Model Including Pipeline Dynamics and Surge". (2011) *Journal of Vibration and Acoustics*, Vol. 133, pp. 051005-1-051055-14.
- [18] Hiradate, K., Sakamoto, K., Shinkawa, Y., Joukou, S., Uchiyama, T. "Investigation on Pressure Fluctuation Related to Mild Surge in Multi-Stage Centrifugal Blower with Inlet Guide Vane". (2015) *Proceeding of ASME TurboExpo*, ASME Paper GT2015-43034, pp. V02CT44A017-V02CT44A017.
- [19] Dumas, M., Vo, H. D., Yu, H. "Post-Surge Load Prediction for Multi-Stage Compressors Via CFD Simulations" (2015) *Proceeding of ASME TurboExpo*, ASME Paper GT2015-42748, pp. V02BT39A022-V02BT39A022)
- [20] Belardini, E., Rubino, D.T., Tapinassi, L., Pelella, M. "Modeling of Pressure Dynamics During Surge and ESD," (2015) *3rd Middle East Turbomachinery Symposium*, Doha, Qatar, February 15-18.
- [21] Biliotti, D., Toni, L., Belardini, E., Vannini, G., Giachi, M., Rubino, T.D. "Stall Induced Aerodynamic Forcing and Rotor Vibrations in a Multistage Centrifugal Compressor". (2015) *3rd Middle East Turbomachinery Symposium*, Doha, Qatar, February 15-18.
- [22] Baldanzini, F., Calosi, M., Belardini, E., Pelella, M., Rubino, T. D., Tapinassi, L., "HPRC Prototype Surge Exploration Tests and Second Quadrant Characteristic Dynamic Modeling". (2016) *45th Turbomachinery & 32nd Pump Symposium*, Houston, Texas, September 12-15.
- [23] Munari, E., Morini, M., Pinelli, M., Spina, P.R. "Experimental Investigation and Modeling of Surge in a Multistage Compressor". (2016) *8th international conference on Applied Energy (ICAE)*. In press, Energy procedia.
- [24] Munari, E., Morini, M., Pinelli, M., Spina, P.R., Suman, A. "Experimental Investigation of Stall and Surge in a Multistage Compressor". (2017), *Journal of Engineering for Gas Turbine and Power*, 139(2), art. no. 022605, DOI: 10.1115/1.4034239.

## *List of Figure Captions:*

**FIGURE 1. MEASURED SURGE FREQUENCY AND FLUCTUATING FORCE VERSUS DOWNSTREAM PIPING VOLUME.**

**FIGURE 2. IMPELLER DAMAGE AFTER SURGE EVENT**

**FIGURE 3. PHOTO OF THE TEST LOOP ARRANGEMENT**

**FIGURE 4. CENTRIFUGAL COMPRESSOR PERFORMANCE MAP**

**FIGURE 5. PROCESSING AND INSTRUMENT DIAGRAM OF THE TEST LOOP WITH ALL RELEVANT DIMENSION**

**FIGURE 6. AXIAL LOAD CELL ON ROTOR THRUST BEARING**

**FIGURE 7. AXIAL VIBRATION FOR NO-SURGE AND SURGE CASE (@ 13,000 RPM)**

**FIGURE 8. DISCHARGE NOZZLE PULSATIONS DURING SURGE @ 10,000 RPM**

**FIGURE 9. SURGE AND NON-SURGE AXIAL FORCES (@ 13,000 RPM)**

**FIGURE 10. FREQUENCY SPECTRUM OF SURGE FORCES (@ 13,000 RPM)**

**FIGURE 11. SURGE AND NON-SURGE AXIAL FORCES VERSUS SPEED**

**FIGURE 12. DIFFERENCE BETWEEN NO-SURGE AND SURGE FORCES VERSUS PRESSURE RATIO**

**FIGURE 13. SURGE PEAK-TO-PEAK VIBRATIONS VERSUS SPEED**

**FIGURE 14. SURGE PEAK-TO-PEAK FORCES CALCULATED FROM DISPLACEMENT DATA**

**FIGURE 15. SURGE FREQUENCY VERSUS SPEED**

*List of Table Captions:*

**TABLE 1. CHARACTERISTICS OF THE COMPRESSOR STAGES**

**TABLE 2. CHARACTERISTICS OF THE INSTRUMENTATION**

**TABLE 3. PERCENT MEASUREMENT UNCERTAINTIES FOR RAW AND REDUCED PARAMETERS**

**TABLE 4. SURGE SEVERITY COEFFICIENT**

**TABLE 5. POTENTIAL DAMAGE**

**TABLE 6. CHARACTERISTICS OF THE COMPRESSOR STAGES**

<b>Characteristics</b>	<b>1<sup>st</sup> stage</b>	<b>2<sup>nd</sup> stage</b>
Rotor max diameter	14.76 in (374.9 mm)	13.26 in (336.8 mm)
Number of blades	9	17
Diffuser type	Vaneless	Vaneless

**TABLE 7. CHARACTERISTICS OF THE INSTRUMENTATION**

<b>Sensors</b>	<b>Type</b>	<b>Uncertainty</b>
Flow meter	Orifice plate	0.2 % FS
Pressure transducers	Membrane	0.1 % FS
Load cells	Strain Gauge	0.3 % FS
Proximity probes	Eddy Current	0.5 % FS
Temperature sensors	Thermocouples	0.1 % FS

**TABLE 8. PERCENT MEASUREMENT UNCERTAINTIES FOR RAW AND REDUCED PARAMETERS**

	$p$	$T$	$Q$	$d$	$N$	$\Delta h$	Thrust Load
Steady	0.3	0.2	0.5	2.0	0.5	0.7	1.5
Transient	0.6	-	-	4.0	-	1.2	3.0

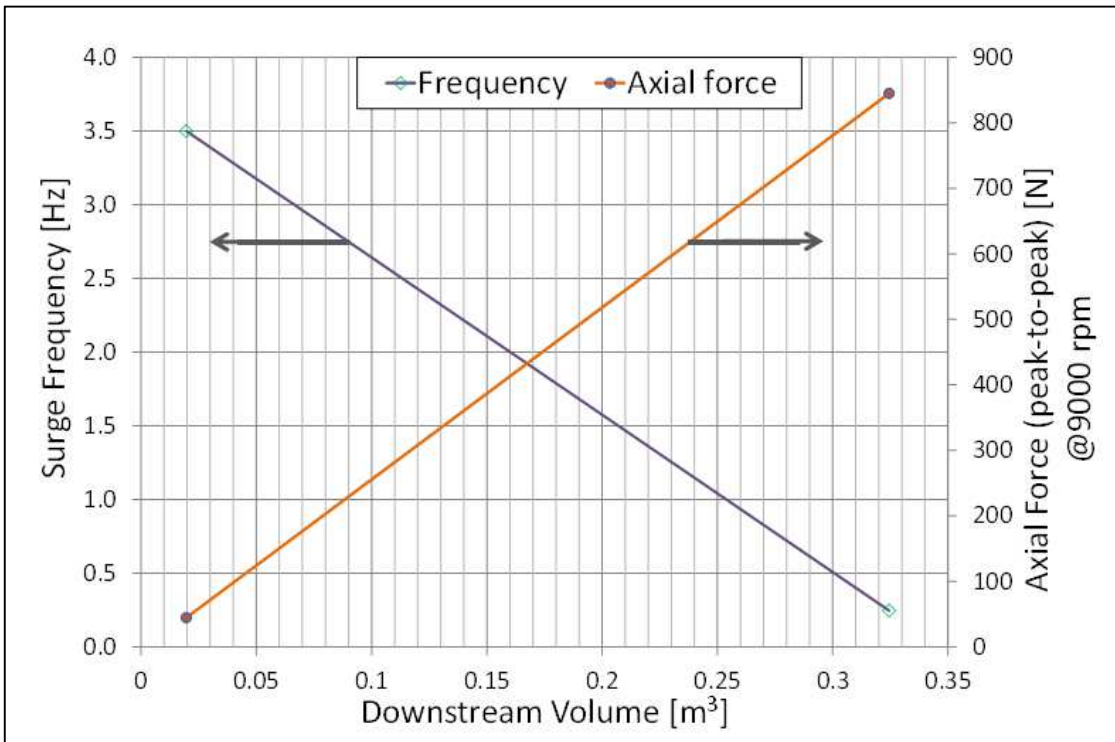
**TABLE 9. SURGE SEVERITY COEFFICIENT**

$N$ [rpm]	$p_d/p_s$ [-]	Force		$\Gamma$ [-]
		[lbf]	[N]	
7,000	1.2	4	17.8	0.000093
9,000	1.34	11	48.9	0.000136
10,000	1.42	10	44.5	0.000154
11,000	1.51	11	48.9	0.000178
12,000	1.62	20	89.0	0.000207
13,000	1.74	25	111.2	0.000243

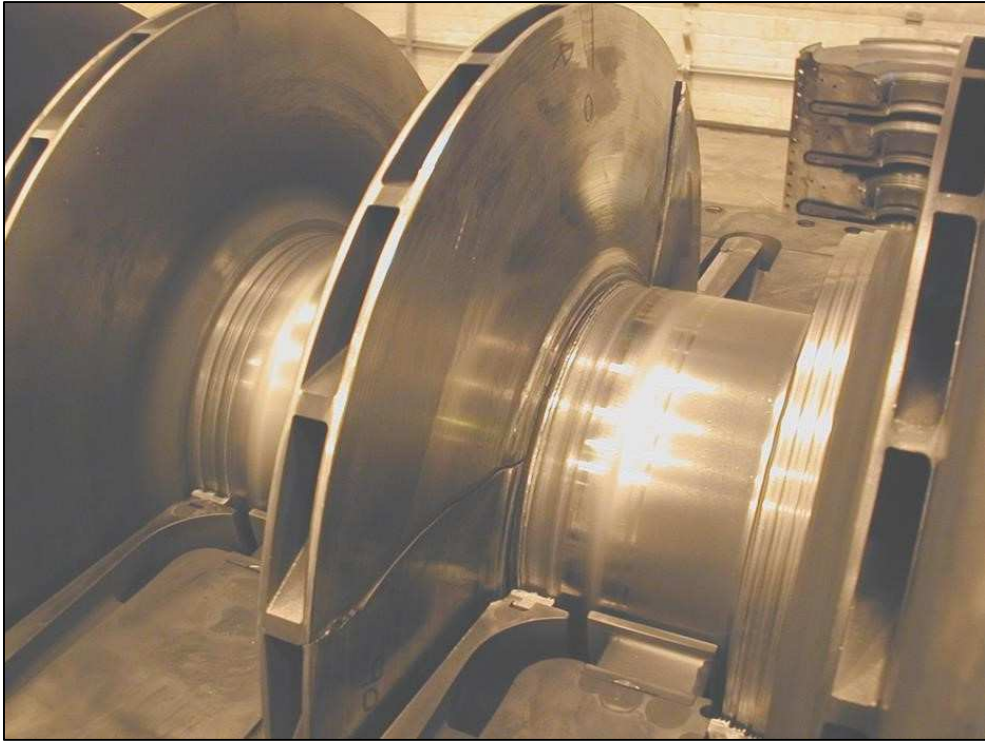
**TABLE 10. POTENTIAL DAMAGE**

$\Gamma < 0.001$	Mild Surge (Low Potential Damage)
$0.01 < \Gamma < 0.001$	Classic Surge (Discrete Potential Damage - Requires Further Analysis)
$\Gamma > 0.01$	Deep Surge (High Potential Damage)





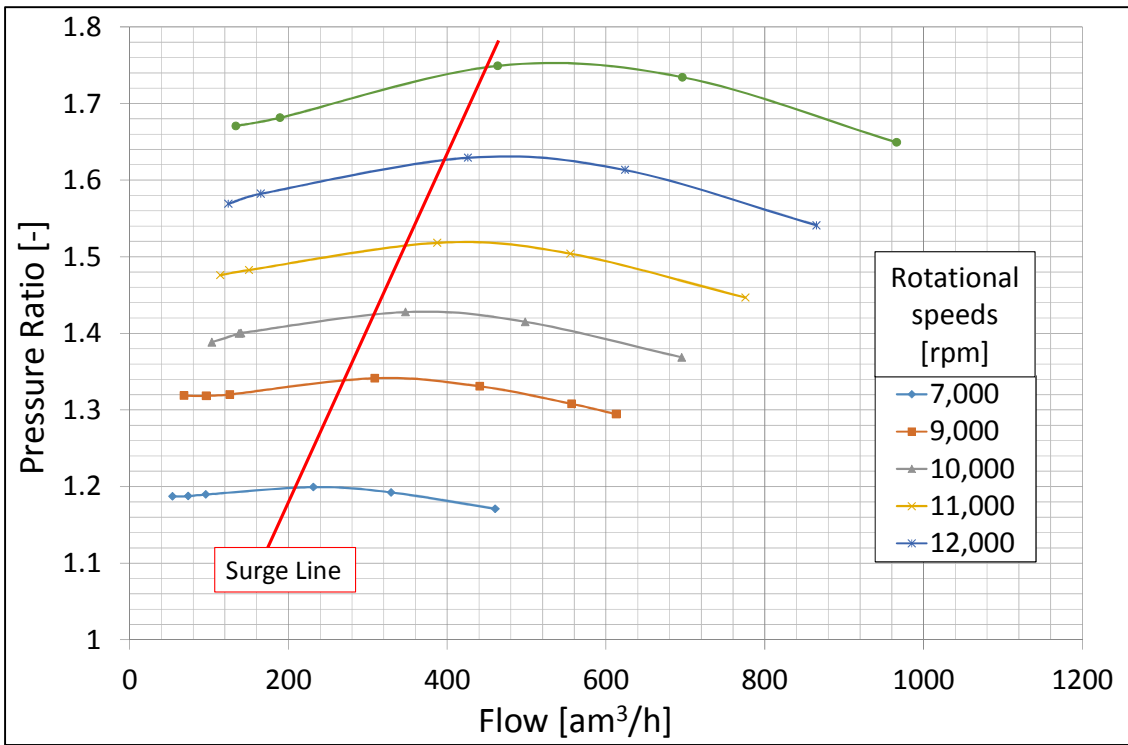
FIGURE\_16\_GTP-17-1223



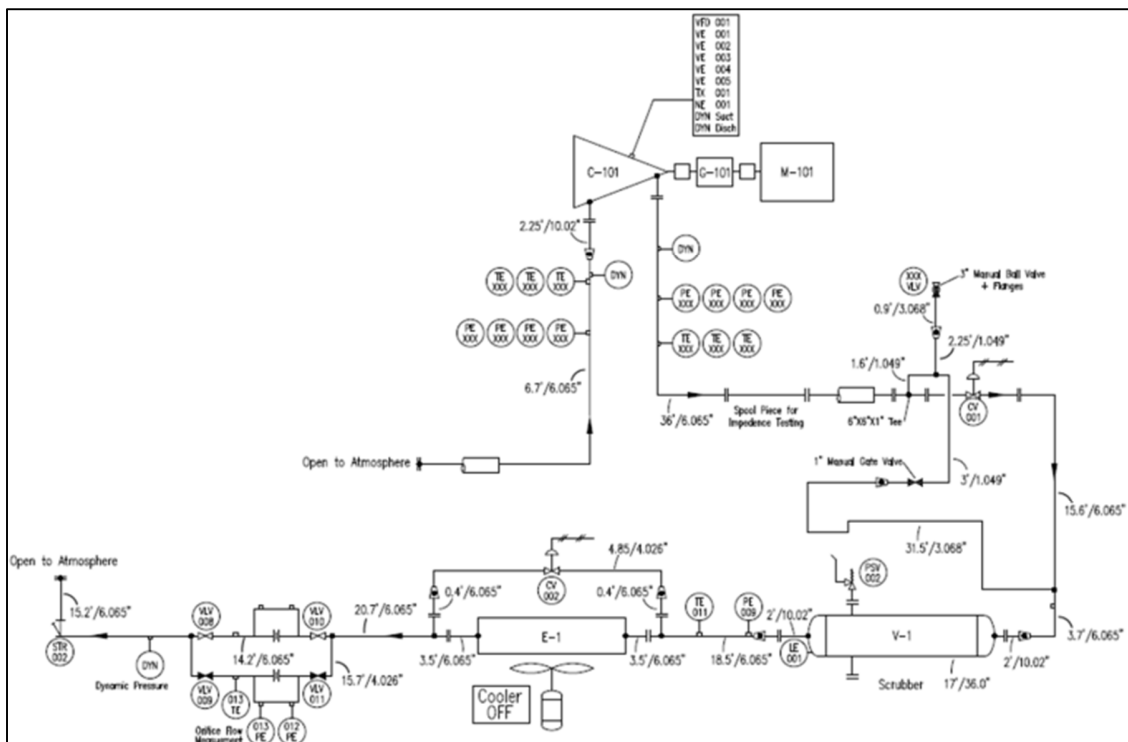
**FIGURE\_2\_GTP-17-1223**



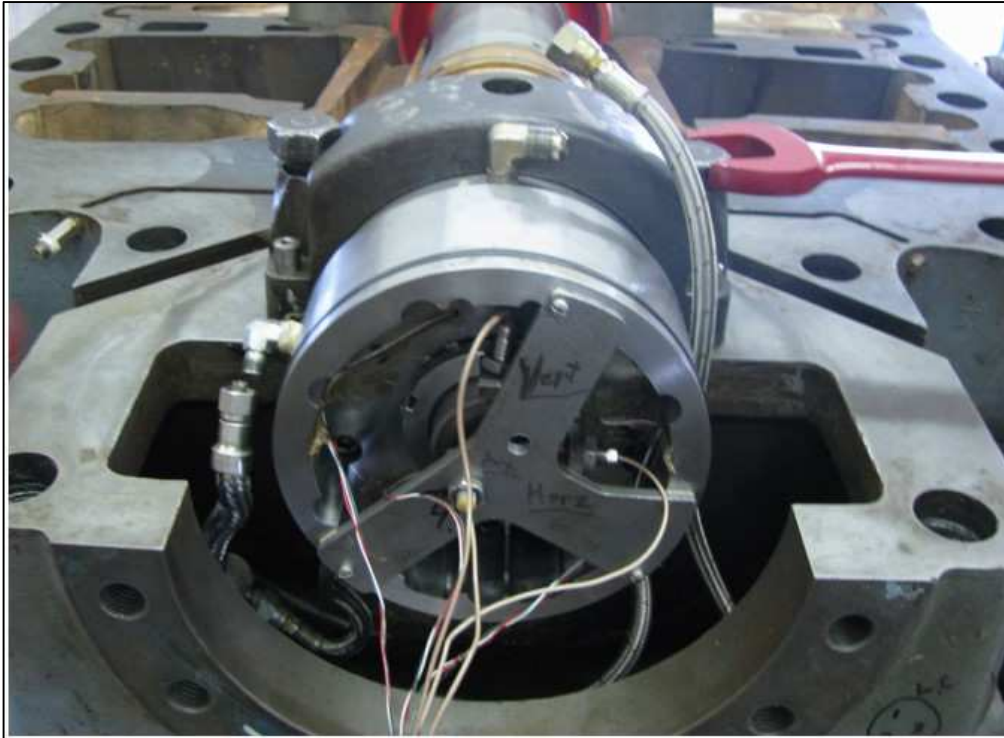
**FIGURE\_3\_GTP-17-1223**



FIGURE\_4\_GTP-17-1223

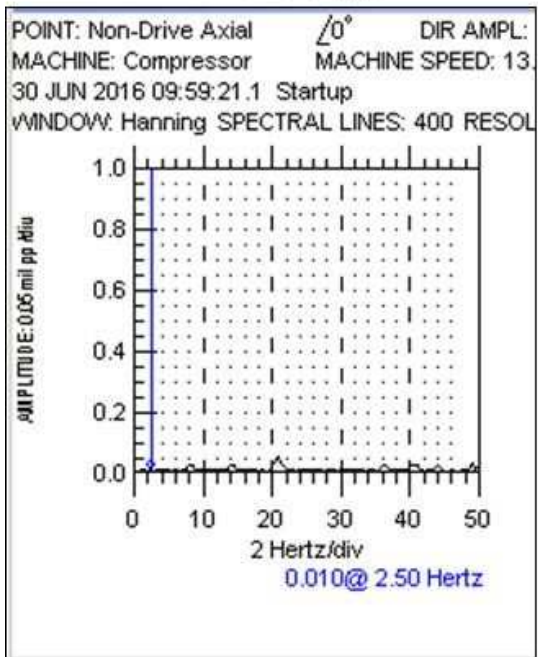


FIGURE\_5\_GTP-17-1223

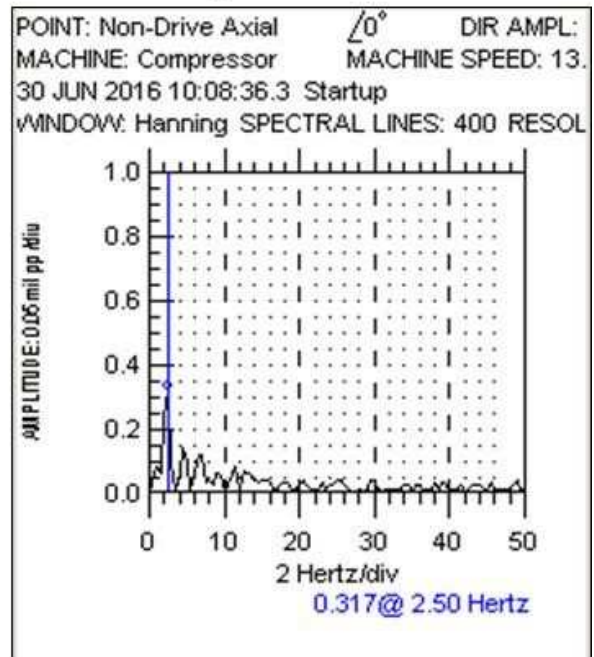


FIGURE\_6\_GTP-17-1223

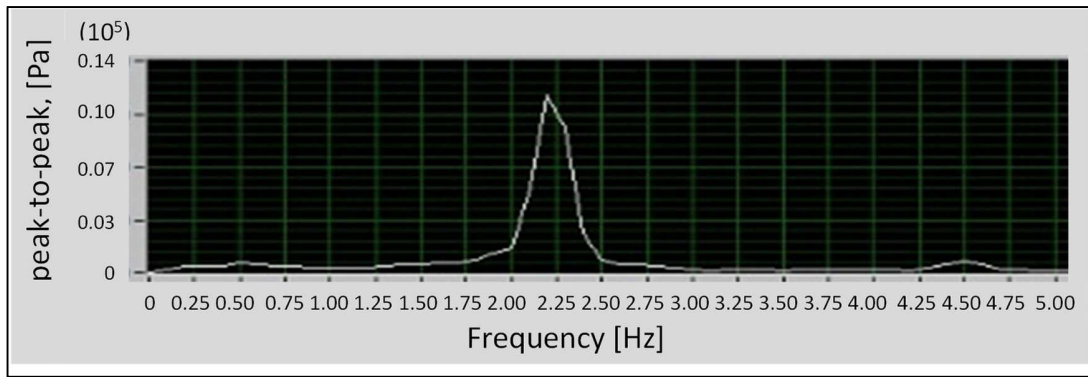
No Surge



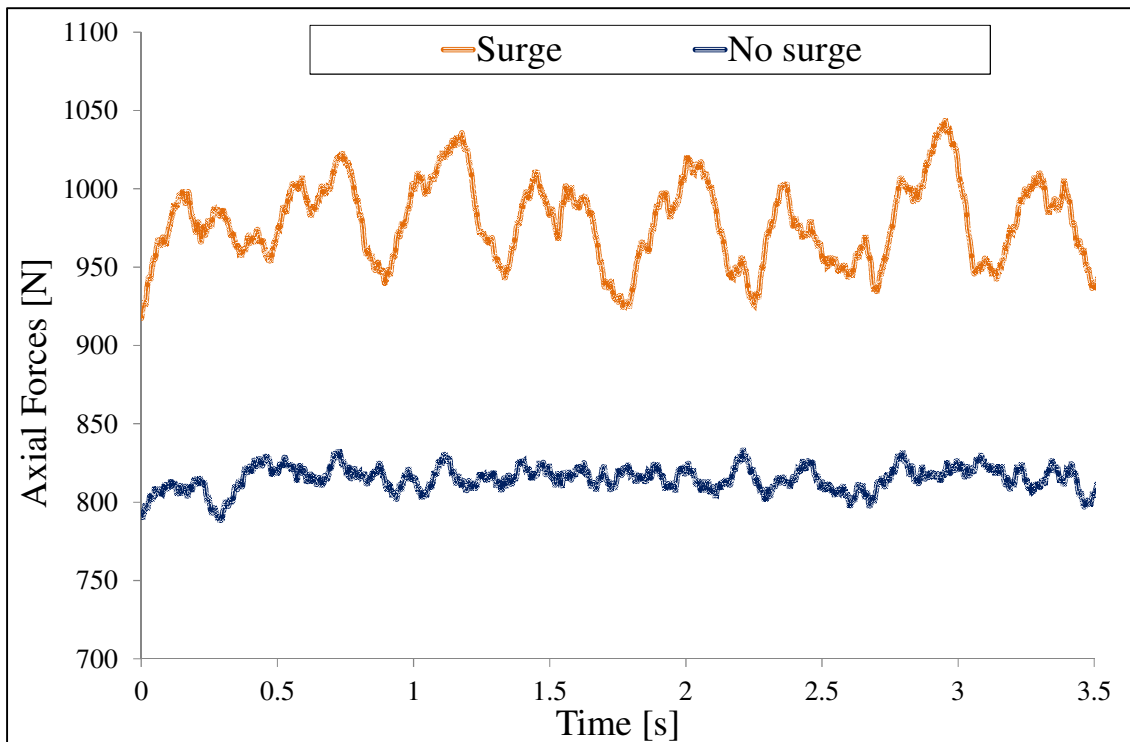
Surge at  $\sim 2.5$  Hz



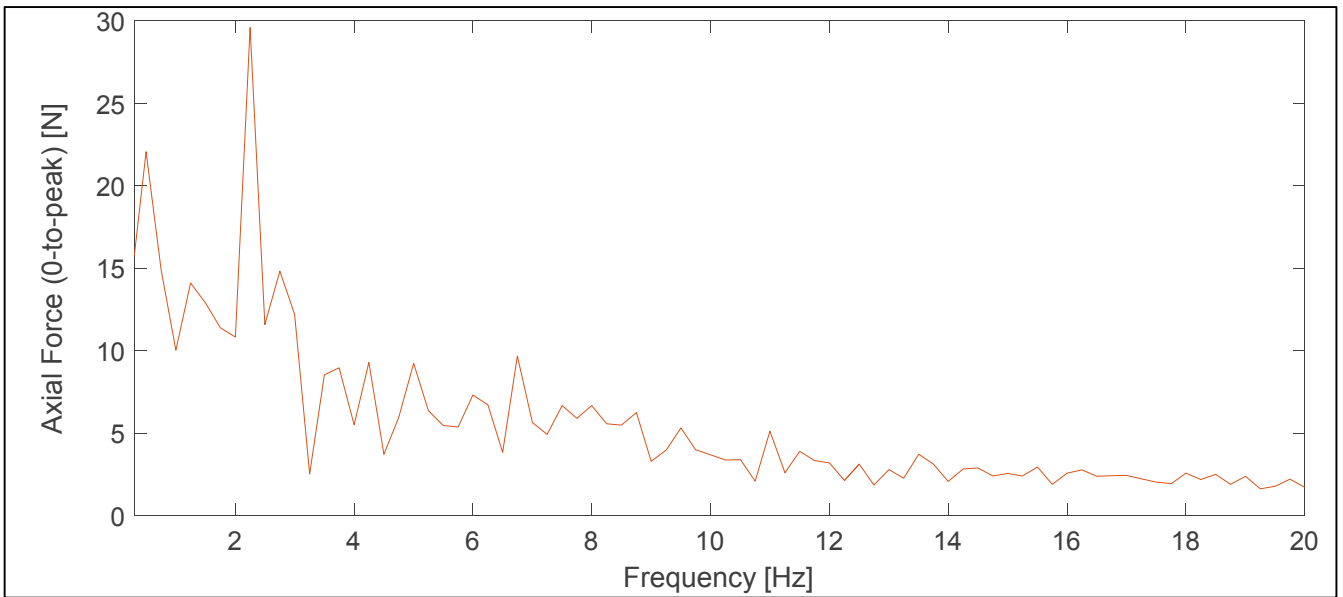
FIGURE\_7\_GTP-17-1223



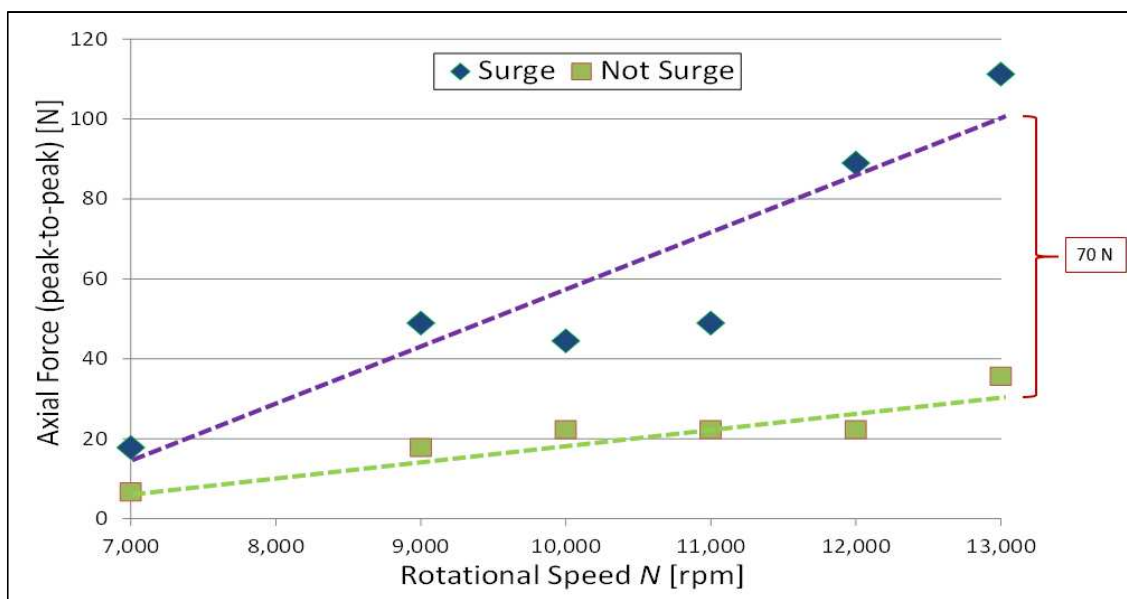
FIGURE\_8\_GTP-17-1223



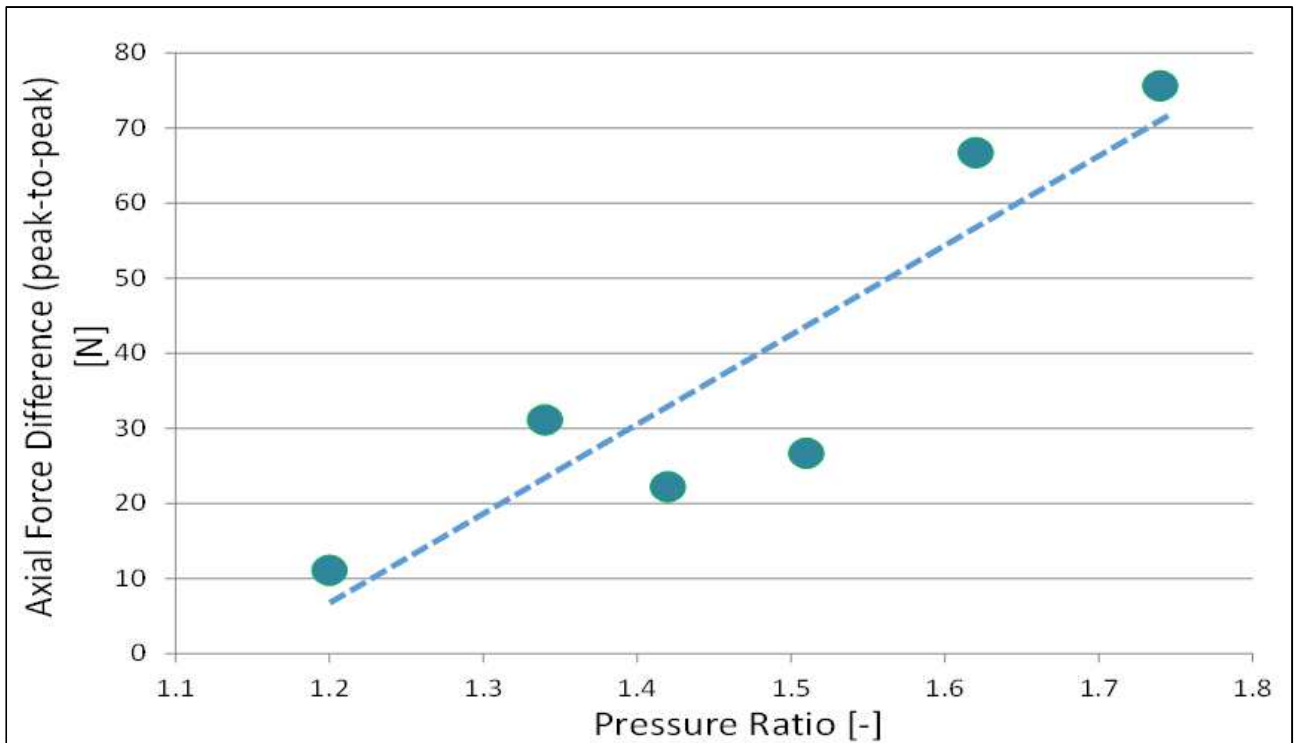
FIGURE\_9\_GTP-17-1223



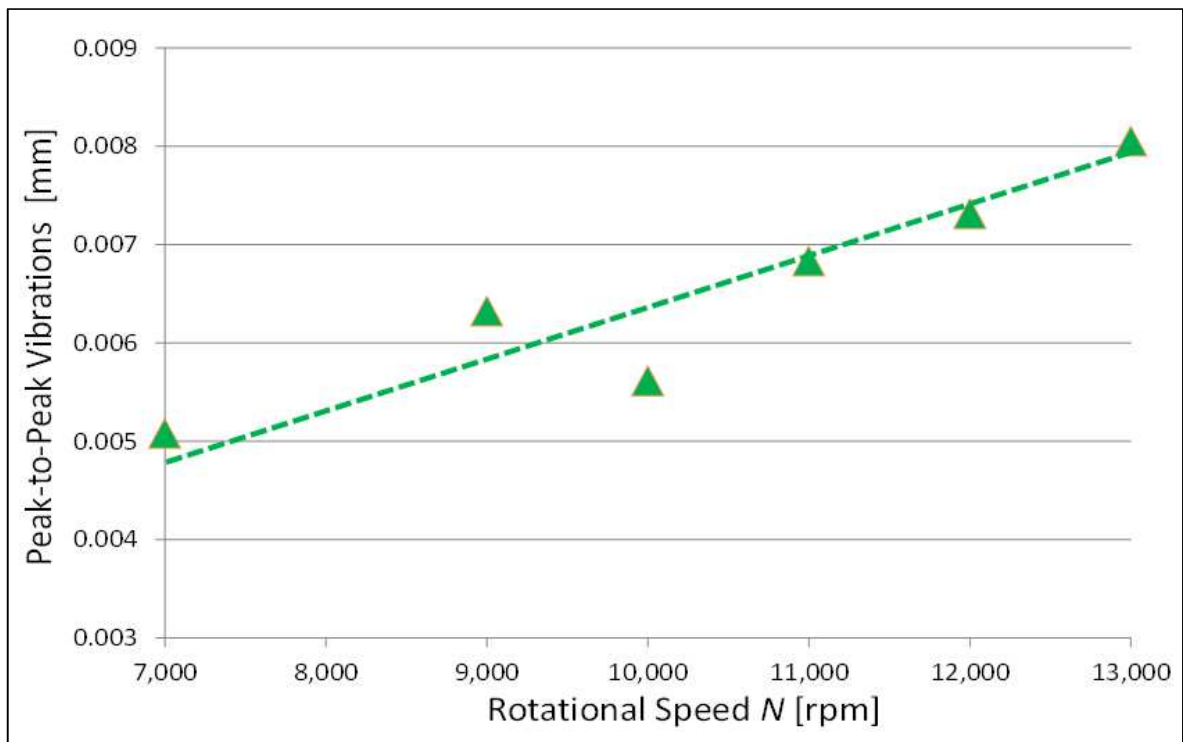
FIGURE\_10\_GTP-17-1223



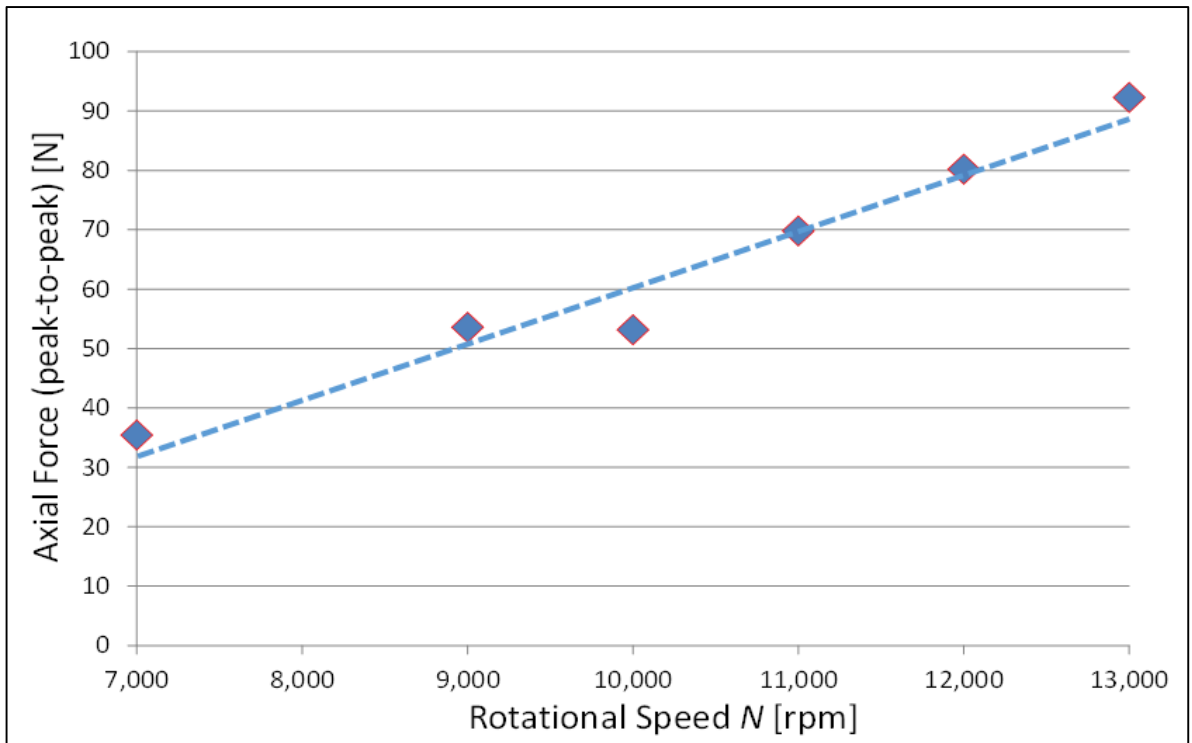
FIGURE\_11\_GTP-17-1223



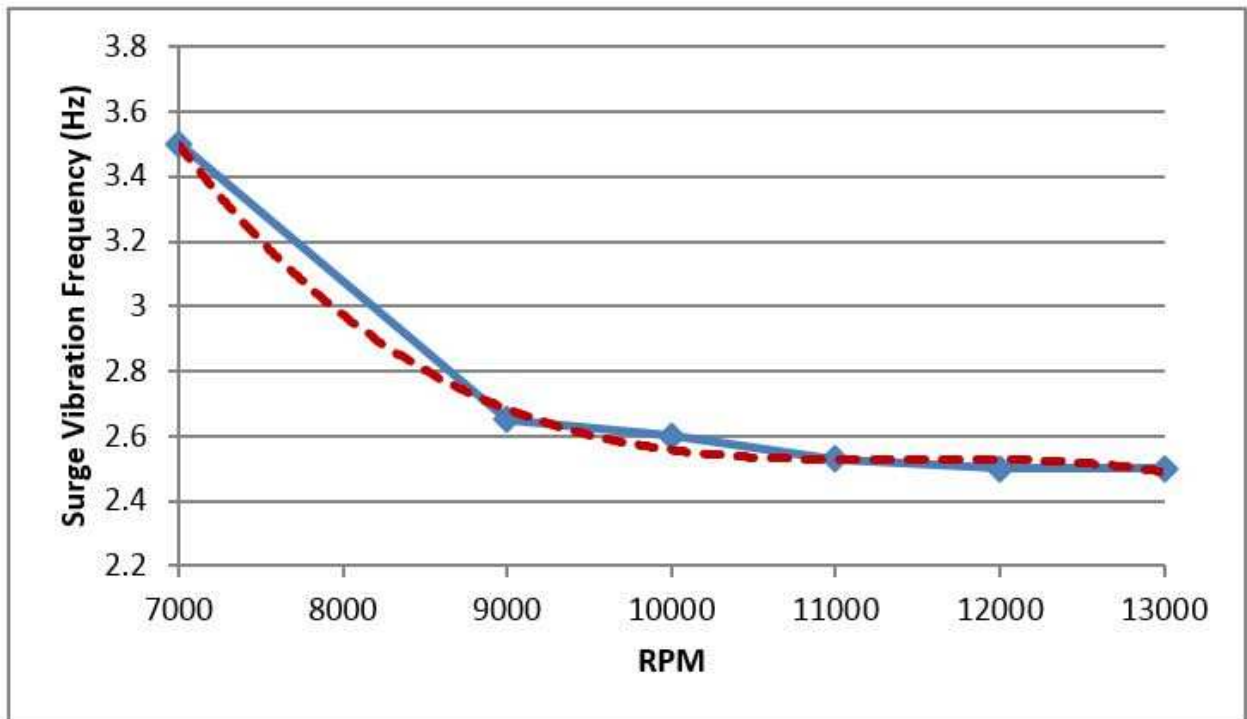
FIGURE\_12\_GTP-17-1223



FIGURE\_13\_GTP-17-1223



FIGURE\_14\_GTP-17-1223



FIGURE\_15\_GTP-17-1223